EVS26
Los Angeles, California, May 6-9, 2012

Evaluation of Lithium Iron Phosphate Batteries for Electric Vehicle under stressful cycling

D. Anseán, M. González, J.C. Viera, V.M. García, J.L. Antuña, H. Corte
University of Oviedo. Campus de Viesques, s/n, Módulo 3, 33204, Gijón, Asturias, Spain.
e-mail: anseandavid.uo@uniovi.es

Abstract

In the past few years, several lithium-ion (Li-ion) technologies have been studied and developed for its use in electric vehicles (EVs). Among these, Lithium Iron Phosphate (LFP) batteries have become a viable choice due to its key features, such as superior intrinsic safety or very large cycle life. As a result of its advantages and the projected impact on the EV market, further studies and tests have to be carried out in order to obtain EVs battery crucial information, such as cycle life, cell safety, reliability or capacity degradation, to name a few. With this aims in mind, this paper presents the results of extensive battery testing procedures conducted on commercial high power LFP cells. A series of relevant combined cycling schemes, which varied from stressful cycling to mixed cycling protocols were carried out for over 5,000 full charge and discharge cycles. Evaluation on important cell parameters such as capacity degradation, cycle life, energy efficiency or cell temperature were performed and then compared with various requirements and targets defined by the United States Advanced Battery Consortium (USABC). The obtained results provide a better understanding of this cell technology, and its performance under the proposed combined stressful cycling.

Keywords: Fast Charge, Lithium Iron Phosphate, Cycle Life, Battery Electric Vehicle

1 Introduction

In recent years, lithium-ion (Li-ion) battery technologies have become a viable choice in energy storage systems, power electric applications and especially significant, the electric vehicle (EV) automotive industry. Nevertheless, a fine variety of lithium-based chemistries are actually being used in EVs and Hybrid Electric Vehicles (HEVs), such as lithium iron phosphate (LFP), lithium nickel cobalt aluminum oxide (NCA) and lithium nickel cobalt manganese oxide (NMC) to name a few [1]. Even though, there is a clear trade-off between energy density and power capability for Li-ion batteries of the various chemistries previously stated [2]. These facts suggest that every Li-ion based cell technology has its advantages and its drawbacks, and no single cell technology stands out from the rest yet.

Among the multiple Li-ion choices available for the EV market, LFP cathode materials have some key advantages over other Li-ion based technologies. These can be summarized in: intrinsic safety and low toxicity, high cycle-lifetime, high-power capability, reliability, large availability of materials, low cost and flat voltage profile [3, 4]. On the other hand, the main issues found with this technology are its lower voltage,

resulting in lower energy density, its poor lithium diffusion and a poor electronic conductivity [5]. However, approaches can be used to overcome the previous two issues, such as the use of nano-structured materials in its chemistry [6].

As a result of its advantages and improved features, LFP batteries are projected to share an important part of the EV market. Consequently, battery and EV manufacturers require extended cycle-life testing studies prior to its commercial implantation. The results of these studies and the obtained information are crucial in terms of safety, reliability, capacity-degradation mechanisms and the practical use of this technology on EVs. Hence, a testing approach is highly recommended to characterize automotive battery cells [7], therefore different testing procedures will be conducted in this work.

Although the driving scheme of an EV may differ radically between users and the region where the EV is being used, there is a set of requirements and targets, defined by USABC [8]. These criteria for advanced battery technologies vary from different values in terms of power density, energy efficiency, among many others. In this paper, special consideration will be given to the long term goals regarding specific power (W/kg), energy efficiency, cycle life and fast recharge time. As a consequence, the cells in this work will be tested under different testing protocols, in order to achieve specific USABC goals. Certainly, some of these test conditions, particularly stressful cycling, could affect the battery functionality. In particular, high currents, high energy throughput and high temperatures are the main factors that force the deterioration of the battery electric characteristics [9].

To recapitulate, this paper is to present and evaluate a series of results obtained from different cycling schemes, tested on commercial LFP cells from the same manufacturer. The proposed tests vary from continuous fast-charging and fast-discharging (stressful cycling) and mixed-type cycling. Since the effects of these proposed cycling tests on the cell degradation remains unknown, investigations will be done by extended cycle-life studies (up to 4,500 cycles) to detect long-term effects on the cells. By monitoring the capacity fade, the efficiencies, the temperature evolution among other parameters, a more accurate evaluation can be done on the tested cells. The results will provide useful information for its potential use in EVs or Battery Management System (BMS) designs, among other applications. Furthermore, the data obtained from the performed tests could be used in follow up studies on cell degradation mechanisms, as reported in [10, 11].

2 Battery test procedures

The A123 Systems ANR26650M commercial low-cost nano-structured LFP cells were selected for this study. These cells are presented by the manufacturer as a high power, versatile and long calendar life battery, suitable for portable high power devices, commercial trucks and bus hybrid electric vehicles (HEVs) [12]. The main characteristics of these cells are summarized in Table 1. Values such as the fast-charge current of 10A (just above 4C) and cycle life need to be emphasized, as these parameters are closely tied to the scope of this paper.

In short, these cells seem to have remarkable characteristics, have a long cycle life and are capable of handle stressful rates, which would not be tolerated by many other cell technologies, such as Cobalt [13].

The experiments were carried out using a multichannel Arbin BT2000 battery testing system (±20A) and the cells were located in a climate chamber from the manufacturer Memmert. The ambient temperature was held at 23ºC during the whole experiment. The temperatures, both in the climate chamber and the cell case were measured with T-type copper-constantan thermocouples and logged into the Arbin System.

Afterwards, the cells were subjected to battery test procedures, developed by the Battery Research Laboratory at the University of Oviedo based on the laboratory's own experience and the study of other renowned international organizations and laboratories [7, 8, 14, 15].

Table 1: ANR26650M1 cell characteristics

A123 Systems	ANR26650M1
Nominal cell capacity and nominal cell voltage	2.3Ah, 3.3V
Internal resistance (10A, 1s DC)	10mΩ typical
Recommended standard charge method	3A to 3.6V CC/CV, 45min
Recommended fast-charge method	10A to 3.6V CC/CV, 15min
Cycle life at 10C discharge, 100% DOD	Over 1,000 cycles
Recommended charge and cut-off voltage at 25ºC	3.6V to 2V
Cell weight	70 grams

2.1 Commissioning

This first stage of the battery test procedure is to identify, weigh and measure the OCVs voltage of the selected cells. The pre-test preparation is then carried out, which requires adjusting all the testing-machine software and hardware in order to achieve better reliability and improve the fidelity and accuracy of the measurements. Planning and scheduling the tests is also taken into account. Once these preparations are finished, the characterization tests begin. The testing plan is shown in Fig. 1.

2.2 Conditioning

Prior to cycling, characterization tests are performed to determine the effective capacity of the testing cells. The standard charging method consists of a constant current stage (CC) at C rate until the voltage of 3.6V is reached, followed by a constant voltage stage (CV) at 3.6V, until the termination current of C/20 is reached. Discharges are performed at constant current C rate, and the cut-off voltage is set to 2V. Both charge and discharge cut-off voltages are the values recommended by the cell manufacturer.

The characterization test sequence consists of performing groups of three different CC discharge cycles. Thus, three cycling at C/3, C/2 and C are performed. For subsequent testing, the battery capacity is considered stable when further three successive C/3 discharges agree within 2% [8]. Once the capacity has been stabilized, a final charge/discharge cycle is performed at C/25 rate. The results of the C/25 measurements provide a practical capacity reference with minimal kinetic effects, close to the maximum capacity attainable [10]. The cells are typically conditioned within 14 cycles.

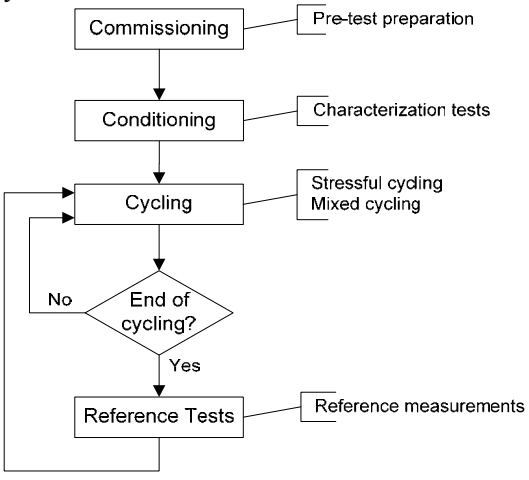

Figure 1: Flow diagram of the testing procedure

2.3 Cycling

Once the characterization tests are finished, the cycling procedure starts. These cycling schemes consist on a series of continuous full charge and discharge cycles (100% DOD) at different rates, depending on the protocol. The proposed cycling protocols are summarized in:

- Stressful Cycling
- Mixed Cycling

Depending on the requirements and planning, these protocols can be maintained from 200 to 400 continuous cycling.

2.4 Reference Tests

After the cycling schemes are finished, reference tests begin. The reference test sequence consists of performing three different CC/CV charge and CC discharge cycles, summarized in:

- Charge C – Discharge at C
- Charge C – Discharge at C/3
- Charge C/25 – Discharge at C/25

This set of tests is used to characterize degradation that occurs during the life of the subject test unit, as well as to measure the internal resistance. The resistance of the cell can be calculated from the difference in IR drops among the C/25, C/3 discharge using Ohm's law; i.e. $\Delta V = R\Delta I$, assuming that the polarization in the cell follows a pseudo Ohmic relationship below C/2 [16].

Reference tests are performed at regular intervals (e.g. every 300 cycles) although the precise number of cycles is particularly specified for every cycling scheme.

3 Cycling protocols

3.1 Stressful Cycling

The stressful cycling consists in performing both fast-charge and fast-discharge on a single cycle. According to USABC, fast-charging is accomplished when a battery is recharged from 40 to 80% of its state of charge (SOC) within 15 minutes [8]. To achieve this goal, several fast-charging methods have been reported [17, 18], although none of the cells used were suitable for EV applications. We developed further studies that show a new fast-charging technique, in which LFP cells can be charged up to 90% of its rated capacity within 15 min, exceeding the USABC goals regarding fast-charge [19]. This fast-charge protocol is the one used in this work.

The fast-charging profile of the stressful cycling is shown in Fig. 2. The charging procedure starts

with a first phase (CC-I) at 4C constant current to 3.6V, followed by second phase (CC-II) at C constant current to 3.6V. The last phase (CV-I) is a constant voltage step set to five minutes of length.

After the fast-charging is accomplished, the fast-discharging procedure starts. It consists in a 4C constant current discharge, until the cut-off voltage of 2V is reached. During the discharge, the specific power delivered by the cell reaches values of 400W kg^{-1}, meeting this long term USABC goal.

Thereafter, the cell is again charged and discharged until the pre-defined cycle number is reached. At this point, a reference test is carried out.

In summary, the stressful cycling consists of a series of continuous fast-charge and discharge profiles. The reference tests will be performed at regular intervals every 300 stressful cycles. The total number of cycles completed using this scheme was 4,500.

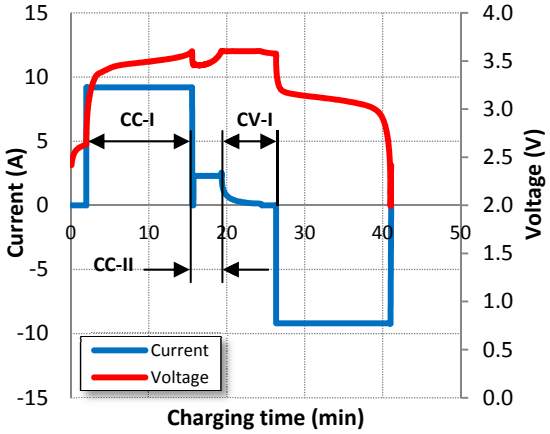

Figure 2: Stressful cycling profile, showing both cell's voltage and current

3.2 Mixed Cycling

The proposed mixed cycling is a compendium of different charge and discharge protocols, carried out on the same cell. Using this approach, which emulates more closely different driving and recharging behaviors, the cell will be evaluated under different charging/discharging conditions throughout several hundreds of cycles, examining long-term effects. Thus, the performance of the cell will depend on the load-history resulting in different capacity fading rates.

The mixed-cycling scheme consists in performing fast discharges, stressful and standard cycles, and fast charges for a determined number of cycles. After each protocol is finished, a reference test is carried out.

Table 2: Mixed-cycling scheme

Test Name	Cycles	Charge	Discharge
Fast-Discharge	0-200	C-CV	4C
Stressful	200-600	4C-C-CV	4C
Standard	600-900	C-CV	C
Fast-Charge	900-1200	4C-C-CV	C

In summary, a total of 1,200 cycles will be completed using this interesting mixed-cycling scheme, which will evaluate the cell under different load conditions. Table 2 recapitulates the cycling schemes that will be evaluated in this protocol, with the charge and discharge profiles used.

4 Results

4.1 Commissioning and characterization results

As the cells are received, the commissioning protocol starts with the weight of the cells. According to the manufacturer datasheets, the cells should weigh 70 g. A precision laboratory scale was used, and Fig. 3 displays the results on four cells from the same batch. The average weight was 73.92±0.46 g (±0.62%), showing that the manufacturing process is accurate.

Fig. 4 presents the effective capacity obtained from the characterization cycles.

The capacity measured at C/25 is the highest and the most consistent, retaining 2.300±0.001 Ah (±0.043%). The capacity at C/3 remains at 2.263±0.017 Ah (±0.751%), whereas the capacity at C is 2.257±0.014 Ah (±0.642%). The cells are rated by the manufacturer at 2.3 Ah at C.

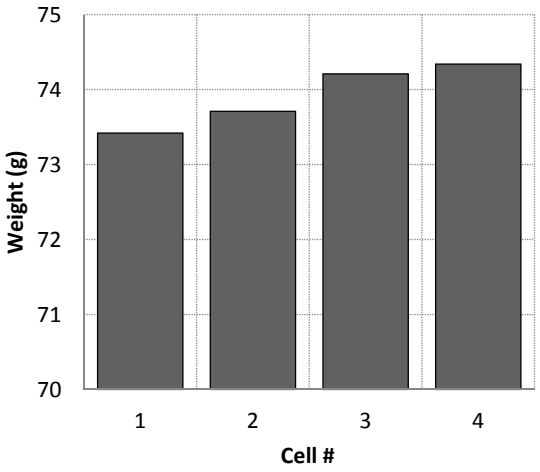

Figure 3: Weight of the cells as received

Therefore, the nominal measured capacity is shorter than 1.8% on average. From these tests, coulombic efficiency was also measured, with values practically invariable, close to 100%. It is worth mentioning that the reproducibility and consistency of the measured capacity and coulombic efficiency under different rates was excellent.

Fig. 5 shows as an example three different cell discharge-rated curves, ranging from C/25 to C. As the area below the curves is proportional to the energy delivered by the cell, it is noticed how the energy at C rate is smaller than at C/25 rate. Even so, the shape of the discharge curves remains similar, and has a convenient flat voltage profile compared with other Li-ion technologies, which are both desirable features.

The average energy delivered by the cells under the characterization tests is shown in the bar chart of Fig. 6. The energy efficiency, calculated from ratio of the net DC energy delivered by the cell to the total DC energy required to restore the initial state of charge (SOC) was 98.90% for C/25, 96.00% for C/3 and 94.95% for the C-rate. These values show a good performance, for a commercial LFP battery.

Finally, based on the average measurements of weight and energy, the cells exhibited a specific energy of 103.1 Wh kg^{-1} at C/25, 99.45 Wh kg^{-1} at C/3 and 98.16 Wh kg^{-1} at C discharging rates. These energy density values are below average, when compared with other Li-ion technologies.

4.2 Stressful cycling results (Cell #1)

The stressful cycling profile for two complete cycles is given in Fig. 7. As it is shown, a full charge and discharge cycle is completed in just 40 minutes. It is also observed that the cell temperature increases rapidly during the discharge. Once the cut-off discharge voltage (2V) is reached, the fast-charge starts. With the first phase at 4C (CC-I), after a slight decreasing, the temperature rises again until approximately the discharge-end values. Then, the last two phases with lower current (CC-II and CV) allow the cell temperature to decrease abruptly to its lower values, next to the thermal chamber preset point (23ºC).

During the whole 4,500 testing cycles, the average cell temperature remained at 26ºC. The maximum temperature values, reached at the end of the discharges were never above 30º, and the minimum went down to 23ºC.

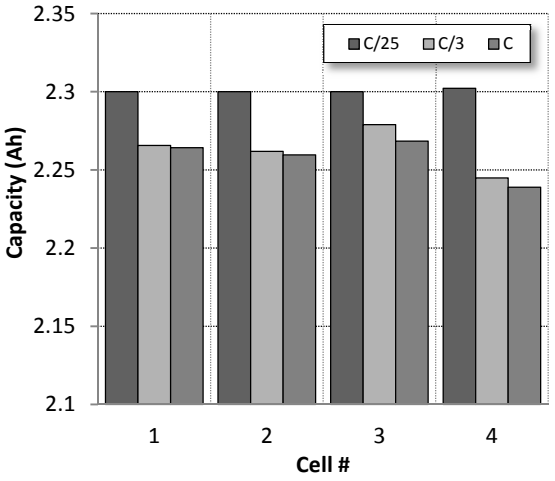

Figure 4: Cell capacities at C, C/3 and C/25

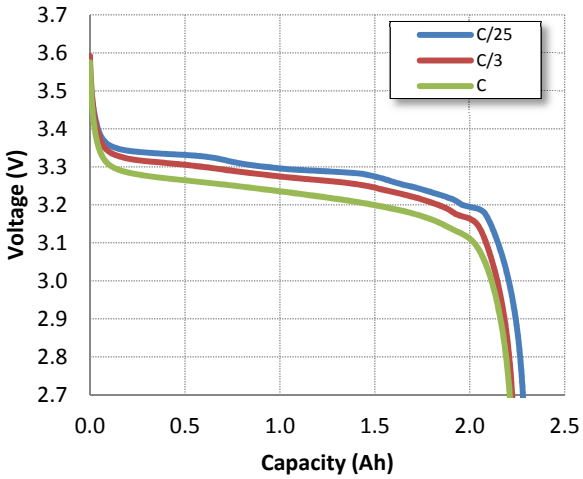

Figure 5: Voltage discharge curves for Cell #1 at different rates from C/25 to C

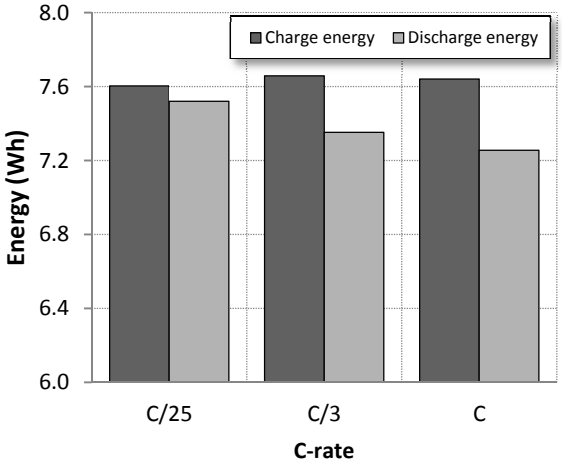

Figure 6: Charge and discharge average energies from C/25 to C

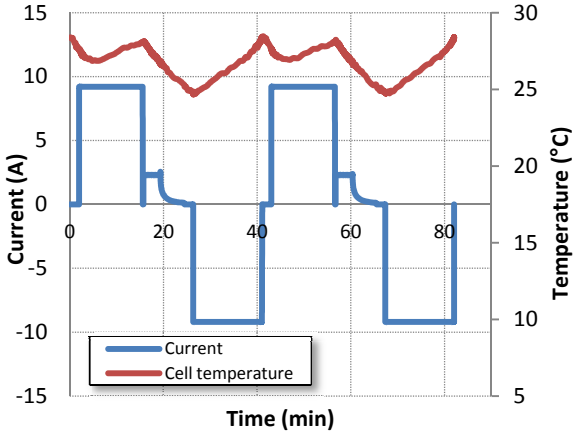

Figure 7: Cell temperature and current evolution during two complete stressful cycles

The evolution of the charged capacity with cycling is shown in Fig. 8. It is observed that nearly all the cell capacity is charged under the first phase CC-I, at 4C. It is remarkable that in just around 13 minutes approximately up to 90% of the cell capacity is filled, even above 4,000 cycles. This performance exceeds the USABC goals of fast-charging. The last two phases (CC-II and CV-I) charge less than 10% of the cell capacity, taking more than 40% of the total charging time. However, as shown before (Fig 7.), these phases allow the cell to decrease its temperature rapidly, while being charged. Thus, it is highly recommended to include this phases to decrease the risk of overheating the cell, avoiding deterioration.

The capacity retention under stressful cycling is shown in Fig. 9. The first cycles reached over 99% of the adopted standard capacity. Then, it is seen that the capacity decreases slightly through cycling.

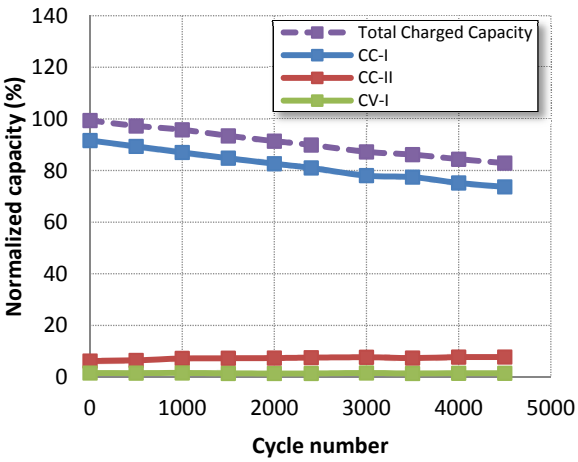

Figure 8: Normalized charged capacity vs. cycle number under stressful cycling

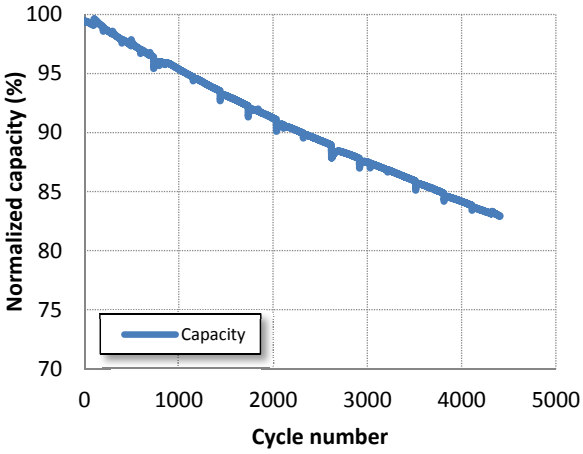

Figure 9: Capacity evolution during stressful cycling

The capacity fade evolution follows a linear trend; about 4% each 1,000 cycles (see Fig. 9.).

Once the predicted 4,500 cycles are reached, the capacity fade was about 17% from its initial capacity. The long term USABC goals for cycle life (80% DOD) are set to 1,000 cycles. Thus, this cell under the proposed stressful cycling successfully exceeds the USABC goals regarding cycle life. Finally, as the capacity fade tendency remains linear, the end-of-life (EOL) is predicted to be reached approximately at 5,200 cycles.

The cell charged and discharged energy is shown in Fig. 10. The ratio of that process (energy efficiency) is also given in the picture. As capacity fade increases with cycling, both charge and discharge energies decrease; even though, as the decreasing rate is the same in both cases, the energy efficiency remains constant through cycling, at around 88%.

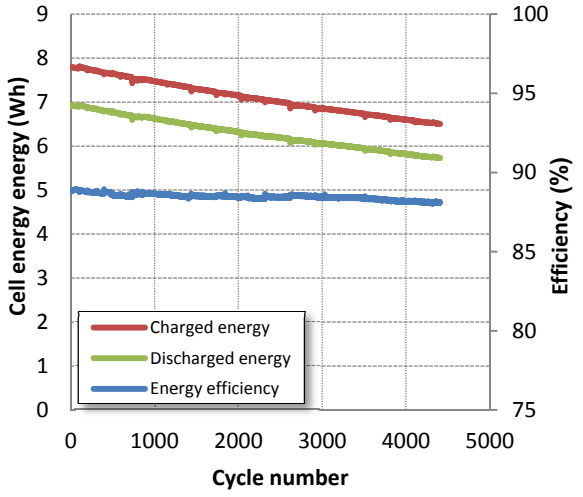

Figure 10: Cell energy and cell efficiency during stressful cycling

Fig. 11. shows the Ragone plot, which reveals the specific energy (Wh kg^{-1}) versus the specific power (W kg^{-1}) delivered by the cell through cycling. This plot shows the trade-off of how much energy is available, and how fast it can be delivered. The data to construct the plot was taken from the stressful cycling and the reference tests.

The curves followed a linear downward trend, with specific energy degradation through cycling. Still, the cell can deliver over 75 Wh kg^{-1} with power demands reaching 400 W kg^{-1} even after 4,500 cycles.

Fig. 12. shows the discharge voltage curves at C and 4C for different cycles. It is noticed how the capacity decreases with cycling practically the same values for both discharge rates. Another interesting result is how these curves, for the same discharge rate, are practically superposed during their flat period. In fact, the discharge voltage values at 4C at 50% SOC for the first cycle and cycle 4,500 are 3.101 V and 3.091 V respectively. These results imply that the internal resistance practically did not change with cycling for a specific discharge rate (less than 1% in 4,500 stressful cycles).

Fig. 12. also shows how the voltage curves at 4C are lower than at C. These curves are directly linked with the energy delivered by the cell, at each specific rate. In fact, discharging at C delivers 5% more energy than discharging at 4C.

4.3 Mixed-Cycling results (Cell #2)

The Cell #2 exhibited a capacity fade evolution as shown in Fig. 13. As it is perceived, there is a sharp difference between the capacity fade tendencies, as a result of the use of different cycling profiles.

From Fig. 13., the first 200 cycles corresponds to the C-CV/4C fast-discharge protocol (1). In this first stage, the capacity retention follows a linear trend with an abrupt negative slope; the capacity fade is 6% from its normalized value, just after 200 cycles. If this tendency had continued, the predicted end of life (EOL) would have been about 1,000 cycles, barely sufficient to meet the USABC goals regarding cycle-life. From cycle 200 to 600 the 4C-C-CV/4C stressful cycling is loaded (2). The slope and tendency of this phase is similar as the previously calculated on Cell #1.

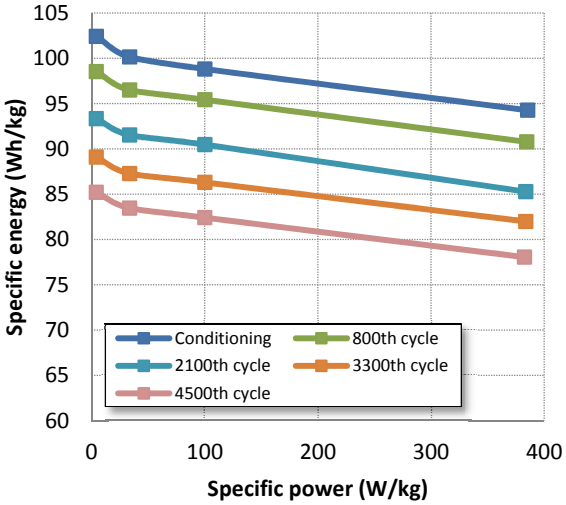

Figure 11: Evolution with cycling of the Ragone plot under stressful cycling

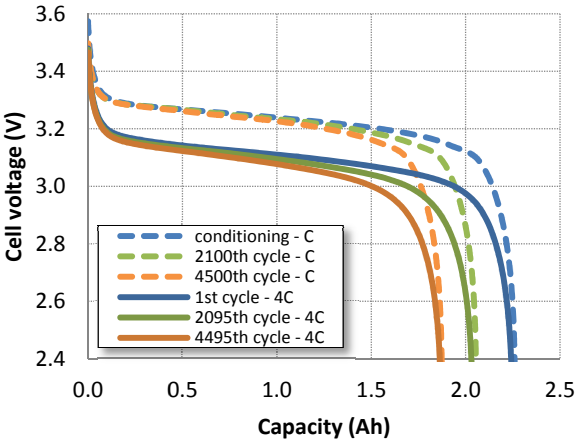

Figure 12: Cell discharge voltage at C and 4C, vs. discharged capacity through different cycles

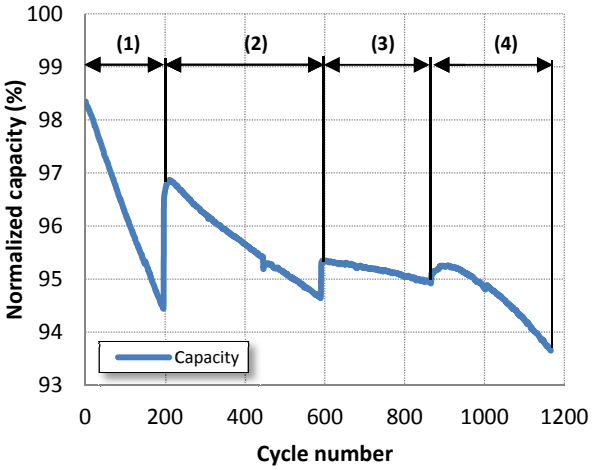

Figure 13: Capacity evolution during the mixed-cycling scheme

A standard C-CV/C protocol was carried out in (3). With this cycling, the cell exhibits an excellent performance, achieving an estimated EOL of 10,000 cycles calculated on its capacity fade slope. The last 300 cycles were carried out with the 4C-C-CV/C fast charge protocol (4). The capacity retention decreases rapidly, and the predicted EOL was calculated to be 3,000 cycles approximately.

Another important fact shown in Fig. 13. is the capacity recovered after each cycling scheme. Depending on the protocol which was used and the one that followed, the capacity recovery varied from 3% after (1) to practically less than 0.5% after (3).

Fig. 14. shows more aspects regarding the capacity recovery and the practical capacity stored in the cell. Testing at C/25 provides a more accurate estimation of the practical capacity in the cell and its progression with aging. It is observed that the tendencies between the two curves are practically parallel in (2) and (3), but there are different slopes in (1) and (4), resulting in a virtual capacity fade higher than the real. In fact, once the reference tests were performed, capacity was recovered abruptly in (1).

The absolute temperature values during cycling are shown Fig. 15. It is seen that the standard cycling has the lowest average temperature (24ºC), while the highest average (26ºC) is reached in the stressful cycling. The fast-charge and fast-discharge protocols have maximum temperatures reaching 28ºC to 29ºC, but the average is a bit lower than stressful cycling (25ºC). Still, the temperature range for the whole experiment is just from 23ºC to 28ºC approximately, even though the cell was subjected to a variety of mixed fast-charge and discharge protocols.

The energy efficiency through the mixed-cycling scheme (reference tests excluded) is shown in Fig. 16. It is observed a direct link between the average cell temperature and the energy efficiency for each protocol. Stressful cycling has both the highest average temperature and the lowest energy efficiency (88%). On the other hand, the standard cycling has both the lowest average temperature and the highest energy efficiency (95%). Fast-discharge and fast-charge protocols have both the medium values of temperature and energy efficiency (91%).

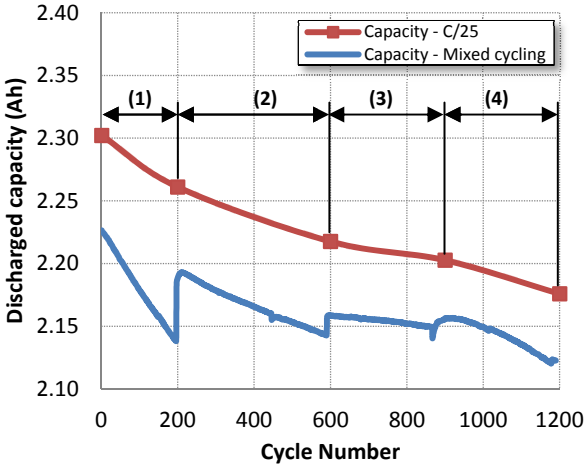

Figure 14: Discharged retention during the mixed-cycling scheme, and discharged retention at C/25 during the reference tests

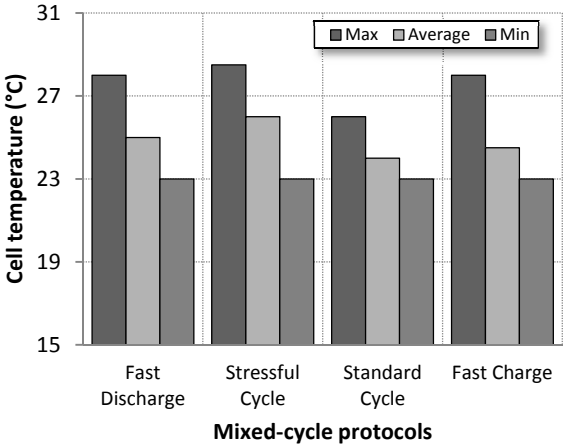

Figure 15: Absolut temperature values during the mixed-cycling scheme

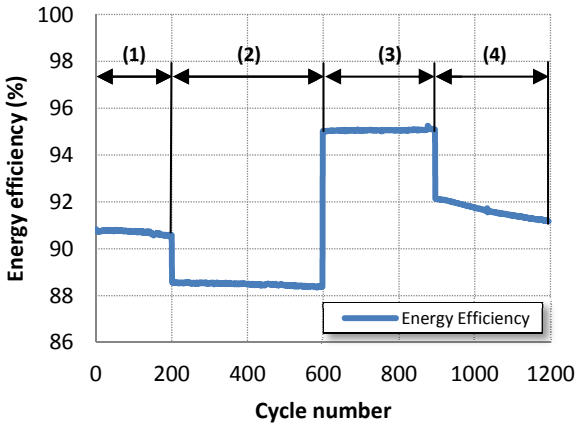

Figure 16: Energy efficiency evolution during the mixed-cycling scheme

5 Discussion

After completing a total of more than 5,700 cycles for both Cell#1 and Cell#2, various aspects can be discussed and analyzed. First, this nano-structured cell technology from A123 Systems, under the proposed tests procedures achieved important USABC long-term goals and exhibited an overall good performance. The main goals are summarized in Table 3. As it is shown, the energy efficiency, the specific energy (for mid - term goal) and the cycle life are met for all proposed testing protocols. Fast-charging is successfully accomplished when the specific fast-charge protocol is used, with more than 90% of the cell capacity recharged in less than 15 minutes. The specific power is only achieved when a fast-discharge (≥4C) is applied. In addition, all the USABC goals can be achieved throughout the cell cycle life. In fact, the stressful cycling meets the proposed goals even after 4,500 cycles. Other experiments on LFP cells have been reported, achieving cycle lives of 1,500 to 2,400 cycles in laboratory tests [20, 21], confirming the good cell performance regarding cycle life.

Regarding the cell temperature, heating through cycling remained constant. This has a direct link with the internal resistance growth: as the internal resistance practically did not increase, the effect on the I^2R losses, were minimal. Thus, the power capability of the cell did not decrease, which is an essential feature in EVs for good driving performance and fast acceleration.

On the subject of specific energy (Wh kg^{-1}), the values were lower than the proposed long term USABC goals, although they met the mid-term objectives. Still, the main drawback for these tested cells is the ultimate price. Even if it is an inexpensive cell, the final price of a system would be over $1000/kWh, whereas the USABC goals set the price at <$100/kWh. Even though wholesale sellers would get a reduced price, nowadays the cost difference would still be huge to meet the price set goals.

Therefore, reducing the battery weight and its final cost are two of the major goals for the wide-spread application of Li-ion batteries in EVs.

Respecting the capacity recovery shown in Cell #2 after the first 200 cycles, some assumptions could be stated: situations such as under-charge (UC) and under-discharge (UD) have been reviewed in similar cycle-life tests, and are likely the consequences of polarization increase in the cell [10, 22]. Even though, this fact can lead to inconsistent calculations on BMSs, as the real capacity loss is smaller than the measured. Hence, reference tests are recommended to be carried out on a regular basis to resolve this issue.

Another interesting result obtained from this work is the variation of the estimated end-of-life (EOL). It is unusual that under a symmetric cycling – same charge and discharge rates as in stressful and standard protocols – the cell performs much better than with anti-symmetric cycling – different charge and discharge rates as in the fast-discharge and fast-charge protocols. Even if the stressful cycling has a higher energy throughput than the fast-charge or fast-discharge protocols, the cell performance under stressful cycling is superior. Although high rate cycling can cause more rapid capacity fade [5, 21] this characteristic was not observed in this work under the proposed cycling conditions.

Regarding Li-ion cell capacity degradation, the main factors have been reviewed elsewhere [5, 11, 23, 24] and can be summarized in: loss of Li inventory, loss of active material, rise of cell impedance and physical degradation. These degradation effects are emphasized at high temperatures, resulting in a significant capacity fade [5, 24]. The various cycling schemes performed on this cell did not increase temperatures abruptly, just below 3ºC on average; therefore, high temperatures were not the cause of degradation in these experiments. In fact, using the proposed fast-charge protocol profile allowed keeping the cell temperature near the ambient temperature.

It is yet early to draw solid conclusions which would help to justify these behaviours, especially regarding the various EOL prediction under anti-symmetric charge/discharge conditions. More experiments and investigations are being developed at our laboratory regarding this subject and the capacity recovery.

Table 3: USABC long-term goals achieved during the testing protocols

Test Name	Specific Energy (Wh/kg)	Specific Power (W/kg)	Cycle Life (cycles)	Fast-Charge (min)	Efficiency
USABC goals	80*	400	1,000	<15	80%
Fast-Discharge	95	400	>1,000	-	91%
Stressful	95	400	>5,000	<15	88%
Standard	98	-	>10,000	-	95%
Fast-Charge	98	-	>3,000	<15	92%

*Mid-term goal

Tests are actually being carried out on more cells from the same batch under various C-rated anti-symmetric charge/discharge conditions, which will help us to explore these issues.

6 Conclusions

In this study, two high power commercial 2.3 Ah LFP cells were tested and evaluated under a series of stressful-cycling testing procedures. The cells succesfully achieved important USABC long-term goals and exhibited an overall good performance, after more than 5,700 cycles in total. The evaluation results showed that the tested cells are safe and can support fast charge/discharge rates without any significant damage for the cycling life. Even though, final cost and specific energy need to be improved for practical and cost-effective EV applications.

Stressful, and mixed-cycle tests in particular, revealed a complicated capacity retention, which is rate and history-dependent. Therefore, reference tests are useful to evaluate the real capacity available on the cell.

The design of appropiate battery testing procedures is essential in order to understand and evaluate the tested-cell behaviour more accurately. Hence, further development and improvements are needed to effectively simmulate and predict the tested-battery performance and capacity fade.

Acknowledgments

The authors would like to thank the Spanish Ministry of Science and Innovation (MICINN) who provided the funding (TEC2009-12552) for this work.

References

[1] C. Pillot, *HEV, PHEV and EV market 2010-2020 impact on the battery business,* European Electric Vehicle Congress, October, 2011

[2] A. Burke, M. Miller, *The power capability of ultracapacitors and lithium batteries for electric and hybrid vehicle applications,* Journal of Power Sources, ISSN 0378-7753, 196 (2011), 514-522

[3] B. Scrosati, and J. Garche, *Lithium batteries: Status, prospects and future*, Journal of Power Sources, ISSN 0378-7753, 195 (2010), 2419- 2430

[4] P. Roth, *Lithium-Ion Cell and Battery Safety*, AABC Europe, June, 2011

[5] W.J. Zhang, *Structure and performance of $LiFePO_4$ cathode materials: A review,* Journal of Power Sources, ISSN 0378-7753, 196 (2011), 2962-2970

[6] A.A. Pesaran, *Choices and requirements of batteries for EVs, HEVs, PHEVs*. National Renewable Energy Laboratory, NREL/PR-5400-51474, April, 2011

[7] G. Mulder et. Al, *Enhanced test methods to characterize automotive battery cells,* Journal of Power Sources, ISSN 0378-7753, 196 (2011), 10079-10087

[8] United States Advanced Battery Consortium. *Electric Vehicle Battery Test Procedures Manual*, USABC, January 1996. http://www.uscar.org/guest/publications.php, accessed on 2012-01-30

[9] M.A. Roscher, J. Assfalg and O.S. Bohlen, *Detection of utilizable capacity deterioration in battery systems,* IEEE Transactions on Vehicular Technology, ISSN 0018-9545, 60 (2011), 98-103

[10] M. Dubarry, B.Y. Liaw, *Identify capacity fading mechanism in a commercial $LiFePO_4$ cell,* Journal of Power Sources, ISSN 0378-7753, 194 (2009), 541-549

[11] J. Vetter et. Al., *Ageing mechanisms in lithium-ion batteries,* Journal of Power Sources, ISSN 0378-7753, 147 (2005), 269-281

[12] A123 Systems, Inc, http://www.a123systems.com/products-cells-26650-cylindrical-cell.htm, accessed on 2012-01-30

[13] K.E. Aifantis, S.A. Hackney, R. Vasant Kumar, *High energy density lithium batteries, materials, engineering, applications,* ISBN: 978-3-527-32407-1, Weinheim, Wiley-VCH, 2010

[14] FreedomCAR battery test manual for power assist hybrid electric vehicles, U.S. Department of Energy, U.S.A., 2003.

[15] Battery test manual for plug-in hybrid electric vehicles, U.S. Department of Energy, U.S.A., 2008.

[16] M. Dubarry et. Al, *Evaluation of commercial lithium-ion cells based on composite positive electrode for plug-in hybrid electric vehicle applications. Part I: Initial characterizations,* Journal of Power Sources, ISSN 0378-7753, 196 (2011), 10328-10335

[17] P. Notten, J. Veld, and J. Beek, *Boostcharging, Li-ion batteries: A challenging new charging concept,* Journal of Power Sources, ISSN 0378-7753, 145 (2005), 89-94

[18] J. Yan et. Al, *Battery Fast Charging Strategy Based on Model Predictive Control,* Vehicular Technology Conference Fall (VTC 2010-Fall), 2010 IEEE 72nd. ISSN 978-4244-3574-6

[19] D. Anseán et. Al, *Fast charge protocol evaluation of lithium iron phosphate batteries for electric vehicles,* European Electric Vehicle Congress, October, 2011

[20] J. Liu et. Al, *Long-term cyclability of $LiFePO_4$/carbon composite cathode material for lithium-ion battery applications*, Electrochimica Acta, ISSN 0013-4686, 54 (2009), 5656-5659

[21] S.B. Peterson, J. Apt, J.F. Whitacre, *Lithium-ion battery cell degradation resulting from realistic vehicle and vehicle-to-grid utilization,* Journal of Power Sources, ISSN 0378-7753, 195 (2010), 2385-2392

[22] M. Dubarry et. Al, *Incremental Capacity Analysis and Close-to-Equilibrium OCV Measurements to Quantify Capacity Fade in Commercial Rechargeable Lithium Batteries,* Electrochemical and Solid-State Letters, ISSN 1099-0062, 9 (2006), A454-A457

[23] K. Striebel, et. Al, *The development of low cost $LiFePO_4$-based high power lithium-ion batteries,* ISSN 0378-7753, 146 (2005) 33-38

[24] M. Dubarry et. Al, *Identifying battery aging mechanisms in large format Li ion cells,* ISSN 0378-7753, 196 (2011) 3420-3425

Authors

David Anseán received the B.Sc. degree in Electronics Engineering from the University of Granada, Spain, in 2007. After gaining some industry experience in Basingstoke, UK, and Berkeley, CA, USA, in 2010 he joined the University of Oviedo, Spain, where he received the M.Sc. degree in Electrical Engineering in 2011, and where he is currently working towards the Ph.D. degree.
His research interests include lithium ion batteries, particularly for its use in electric vehicles.

Manuela González received the M.Sc. and the Ph.D. degrees in Electrical Engineering from the University of Oviedo, Spain, in 1992 and 1998, respectively. She is the founder and head of the Battery Research Laboratory in the Department of Electrical and Electronic Engineering, at University of Oviedo.
Her research interests include battery management systems for new battery technologies and fast chargers for traction applications.

Juan Carlos Viera received the M.Sc. degree in Electrical Engineering from the University of Technology (ISPJAE), Havana, in 1992 and the Ph.D. degree in Electrical Engineering from the University of Oviedo, Spain, in 2003. He is currently an Assistant Professor in the Department of Electrical and Electronic Engineering, at the University of Oviedo, Spain.
His research interests include battery management systems, battery testing, fast-charging among others.

Víctor Manuel García is Professor in the area of Physical Chemistry at the University of Oviedo, Spain, with a doctorate in Quantum Chemistry and expertise in Theory of Electronic Separability.
For several years his research interest has been focused on applied aspects of electrochemistry, either in batteries or corrosion. His research is coupled with an intense dedication to chemical education.

José Luis Antuña received the M.Sc. in Industrial Electronic Engineer from the University of Oviedo, Spain, in 2007. He had a working grant at HC energy company during 2008. He also worked as researcher recycling industrial waste at School of Mines in 2009 and 2010. He is currently working towards the Ph.D. degree and as a researcher at the Battery Research Laboratory at University of Oviedo.

Héctor Corte received the B.Sc. in Physics from the University of Oviedo, Spain, in 2010. He is currently working with the Battery Research Laboratory at the University of Oviedo and towards the M.Sc. in Physics of Complex Systems at the National Distance Education University (UNED).
His work is mainly focused in modelling and mathematical study of the batteries.